Mateusz TAŃSKI [1], Robert BARBUCHA[1], Marek KOCIK[1], Katarzyna GARASZ[1], Jerzy MIZERACZYK[1,2]

Szewalski Institute of Fluid-Flow Machinery (1), Gdynia Maritime University (2)

Diagnostics of UV Nanosecond Laser Generated Plasma Plume Dynamics in Ambient Air Using Time-Resolved Imaging

Abstract. *The dynamics of UV nanosecond laser generated ablation plasma plume expanding in ambient air was investigated. The time-resolved images of the forming and expanding ablation plume were captured. Using the captured images the initial velocity of the plasma was found to vary from $6 \cdot 10^3$ m/s to $7 \cdot 10^3$ m/s depending on the laser pulse fluence. The plasma expansion parameters obtained by us were compared with those predicted by shockwave model and drag model. It was found that drag model better describes plasma expansion in our experiment.*

Streszczenie. *W artykule przedstawiono wyniki badań rozszerzania się w powietrzu plazmy ablacyjnej generowanej ultrafioletowym nanosekundowym impulsem laserowym. Badania polegały na wykonaniu zdjęć plazmy ablacyjnej w technice wysokiej rozdzielczości czasowej. Z analizy otrzymanych zdjęć wynika, że początkowa prędkość rozszerzającej się plazmy ablacyjnej wynosi od $6 \cdot 10^3$ m/s do $7 \cdot 10^3$ m/s w zależności od natężenia promieniowania laserowego. Porównano parametry rozszerzania się plazmy ablacyjnej z dwoma modelami teoretycznymi: modelem fali uderzeniowej (shockwave model) i modelem hamowania (drag model). Okazało się, że model hamowania lepiej opisuje zjawisko rozszerzania się plazmy ablacyjnej w naszych warunkach eksperymentalnych. (**Badanie dynamiki plazmy ablacyjnej generowanej za pomocą nanosekundowych nadfioletowych impulsów laserowych techniką obrazowania w wysokiej rozdzielczości czasowej**)*

Keywords: plasma, dynamics, timer resolved imaging, laser ablation
Słowa kluczowe: plazma, dynamika plazmy ablacyjnej, obrazowanie w technice wysokiej rozdzielczości czasowej, ablacja laserowa

Introduction

The nanosecond laser ablation has many applications, such as laser micromachining, pulse laser deposition (PLD), nanoparticles and clusters formation, and material sampling for spectroscopic analysis (LIBS) [1-3]. When a high-energy nanosecond laser pulse is impinges onto the material surface, a small portion of this material can ablate due to fast temperature and pressure rise. The ablated highly ionized material forms expanding plasma cloud, called a plasma plume. The expansion mechanism of laser generated plasma plume is not fully understood. It involves processes like: deceleration of the plasma plume constituents, shock-wave formation, heat transfer, ion recombination and clustering on their paths through ambient air [4,5]. Generally, the early stage of interaction of the laser pulse with metal target and plasma formation can be presented as four stage process: absorption of the laser energy by the target matter and the energy conversion to heat; the matter evaporation and formation of the plasma plume; absorption of the laser energy by the plasma plume in the shielding process during the plasma expansion; and the plasma plume decay. The dynamics of the laser generated plasma plume depends strongly on following parameters: laser pulse energy, laser beam wavelength, laser pulse duration, target material and pressure of the ambient gas [6,7]. Parametric studies of the plasma plume dynamics such as its expansion rate, size of the plasma plume and decay time are helpful for the optimization of the ablation processes. Therefore the dynamics of plasma plume generated by the nanosecond laser pulses was parametrically studied by several groups. For example, Toftmann et al. [5] measured the plasma dynamics for different laser spot geometries. Elhassan et al. [8] and Joshi et al. [9] studied the influence of the external electric field and magnetic field on the plasma plume dynamics, respectively. However these works were focused on the application of laser generated plasma for material sampling or laser deposition, where the applied laser fluence was relatively low and the ablation took place in vacuum or in gases at a low pressure. The reports on parametric studies of the plasma plume expansion where the ablation is used for laser micromachining (with a moderate laser fluence, in ambient air at atmospheric pressure) are scarce [10-12].

To understand the mechanism of laser generated plasma plume expansion, the two dimensional, time-resolved imaging technique has often been applied [13,14]. Using also this technique, we performed an experiment in which the dynamics of a UV laser generated plasma plume expanding in ambient air was investigated at the early stage of its expansion (first 100 ns). The ablation plasma plume was generated by focusing a UV laser beam onto the surface of a thin stainless steel foil. The time-resolved images of the forming and expanding plasma plume were captured at the intervals of a fraction of nanosecond. Using the captured images the expansion parameters of the plasma were determined.

Experimental Setup

The experimental setup used for the ablation plasma dynamics measurements is presented in figure 1. It consisted of a laser system for plasma generation and a system for plasma observation using a fast gated ICCD (Intensified CCD) camera.

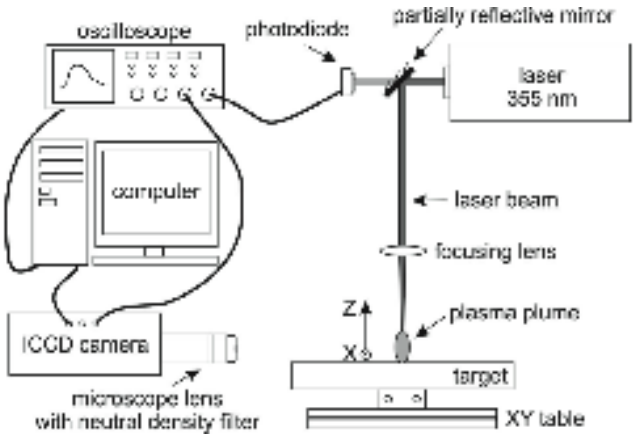

Fig.1. Experimental setup for time-resolved imaging of the laser generated plasma plume

The main elements of the system for plasma generation were:

- a UV laser (solid state laser with third harmonic generation Nd:YVO, wavelength λ = 355 nm, maximal averaged power P = 6 W, laser pulse duration τ = 55 ns, laser pulse repetition rate f = 28 kHz),
- a focusing lens (of a focal length f = 100 mm),
- an XY table with a metal-foil target.

The target used in this experiment was a 304 stainless steel foil of a thickness of 200 μm. The laser beam was directed perpendicularly to the target surface (along Z axis) and focused with the lens. The laser spot on the target surface was d = 20 μm in diameter. Using this system, a few-hundred-micrometer long plasma plume was generated above the target surface with each single laser pulse. After each laser pulse the target was shifted horizontally to avoid double-shooting the pulse onto the same spot. Thus, each laser pulse interacted with untreated target surface. In order to reduce the laser beam power, UV absorbing attenuators of various thickness were introduced into the path of the laser beam. The laser pulse energy was determined as the ratio of the average laser beam power to the laser pulse repetition rate. The plasma plume was generated with the laser pulses producing a laser energy fluence from 30 J/cm^2 to 50 J/cm^2 on the target, which is typical for the laser micromachining processes. The laser pulse shape is presented in the figure 2.

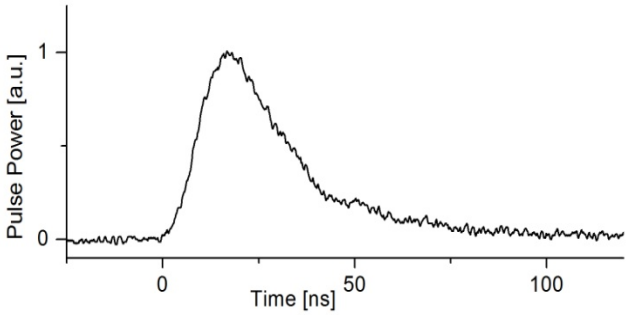

Fig. 2. Laser pulse shape

The system for plasma observation consisted of a fast gated ICCD camera (2 ns of the minimal exposure time, or gating time) equipped with a microscope glass lens and a time synchronization unit. In the front of microscope lens a neutral density glass filter was placed to control the intensity of plasma-emitted reaching camera sensor. This protected the ICCD camera against damaging. The glass filter cut-off the stray UV laser light headed towards the microscope lens. The microscope glass lens and neutral density glass filter reduced the recorded spectra of the plasma plume emission to the visible range. The ICCD camera was focused onto the central region of plasma plume formation (a side view). The observation area was 1.9 mm × 1.9 mm and the captured images resolution was 1.8 μm/px.

ICCD camera exposure (gating time) time was fixed at 2 ns for each captured image. The camera exposure was triggered with the laser trigger signal formed by the time synchronization unit. The delay time between the laser trigger signal and camera exposure could be changed. This allowed capturing the images at various time delays with respect to the ablating laser pulse. The laser pulse signal was detected using a fast photodiode (less than 1 ns rise time). Both the laser pulse signal and camera exposure signal were monitored on an oscilloscope. The delay time between laser pulse and camera exposure was precisely determined using an oscilloscope build-in function. Simultaneously with each captured image of the plasma plume, the delay time was automatically transmitted to the computer. Images of the creating and expanding plasma plume were captured as an event sequence in 500 ps intervals after the laser pulse onset.

The measurements were performed in ambient air under the standard conditions (T = 25°C, P = 1 atm.) in absence of any assisting gas.

Results

Typical ICCD images of the plasma plume at the early stage of its expansion (from 4 ns up to 77 ns) are presented in figure 3, in which the metal-foil target is located at the bottom of the images and the laser beam came from the top.

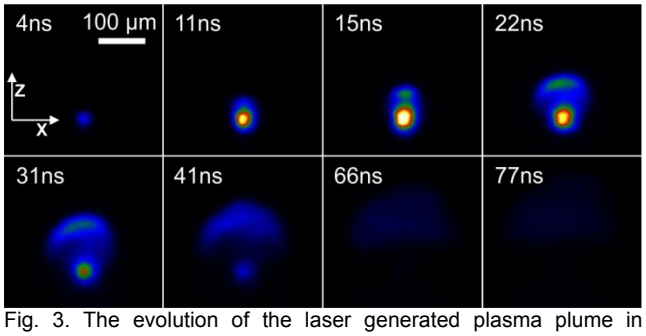

Fig. 3. The evolution of the laser generated plasma plume in ambient air at the early stage of its expansion. Images were recorded using an ICCD camera (exposure time 2 ns). Laser pulse duration τ = 55 ns, laser pulse fluence = 52 J/cm^2.

The captured images reveals that the formation of the plasma plume starts just after the laser pulse onset in the form of a high-temperature spot on the surface of the metal-foil target. Then, plasma expands both quasi-hemispherically in vertical (Z) and horizontal (X) directions, resembling a mushroom-like explosion. The expansion of the plasma is caused by pressure difference between the hot ablation zone, where the laser pulse energy is primarily absorbed, and the ambient air. The expanding plasma plume absorbs a part of the incoming laser pulse energy, in the so-called plasma shielding effect. The expanding plasma prevents the laser energy from being transmitted to the target. At the end of the laser pulse (around τ = 60 ns) the plasma plume is fully developed, while the plasma spot on the target surface disappears. After the laser pulse the plasma plume starts to decay and eventually its intensity reaches the detection limit of the ICCD camera.

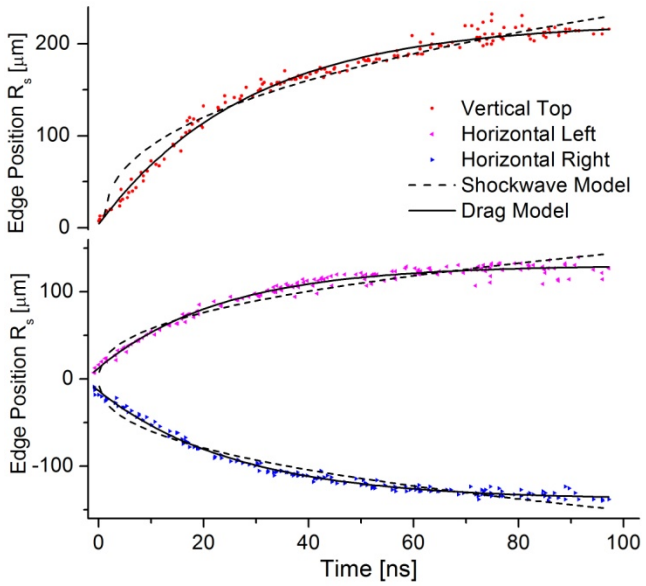

Fig. 4. Plasma plume edge positions as a function of time in vertical and horizontal directions. Laser pulse duration τ = 55 ns. Laser fluence = 52 J/cm^2. Points – experimental results, dashed and solid lines – calculated according to the shockwave and drag models, respectively.

The captured images were used to determine the positions of the vertical leading (top), left and right

horizontal edges of the expanding plasma plume as a function of time. The edges of the plasma plume were defined as the places in the image where the plume intensity is 0,5 % greater than that of the background. Figure 4 presents the vertical (top) and horizontal (left, right) edge positions of the plasma generated by the laser pulse of a fluence of 52 J/cm^2. It is worth mentioning that each experimental point in figure 4 was obtained for a different plasma plume, however, induced by the same laser pulse fluence. Since initial parameters of a series of the plumes induced using the same fluence could vary, each plume evolved slightly differently.

The expansion of the ablation plasma plume is usually described with two models: the shockwave model [15] and drag model [16]. In the shockwave model the expansion of the plasma plume with supersonic velocity creates a sudden pressure rise in the ambient air, which in consequence generates a shockwave that precedes the plasma. It was shown [17,18] that the shockwave and the plasma plume edge both expand with similar velocity. Therefore the expansion of the plasma plume can be described by the shockwave propagation theory. According to this theory, the expanding shockwave front position R_s changes in time t as follows:

$$R_S = \xi_0 \left(\frac{E}{\rho_0} \right)^{\frac{1}{5}} t^{\frac{2}{5}} \tag{1}$$

where ξ_0 is a constant which depends on the specific gas heat and is close to one, E is the laser pulse energy, ρ_0 is the density of the ambient gas.

The experimental data points in figure 3 were fitted with curves resulting from equation (1). It can be seen that the shockwave model curves fit reasonably well the experimental points in the time-range measured. However, in the shockwave model the plasma plume expands to the infinity with increasing time. Hence this model is usually applied to the plasma plumes generated in vacuum or at very low-pressure ambient gas, where practically there is no gas molecules that would stop the plasma expansion.

From the observation (figure 4) we figured out that plasma plume in air at atmospheric pressure expands fast at the beginning of the laser pulse and it slows down until it reaches an expansion limit (also called the stopping distance) and starts to decay. This deceleration of the plasma plume edge is caused by the air molecules that creates the drag force for the plasma. This phenomenon is taken into consideration in the drag model, where the plasma edge approaches asymptotically the expansion stopping distance. In the drag model the plume edge position R_s is given by the equation:

$$R_S = R_{max}\left(1 - e^{-\beta t}\right) \tag{2}$$

where R_{max} is the stopping distance of the plasma plume edge, and β is the slowing coefficient.

Figure 4 shows that the drag model describes the evolution of the plasma plume better than the shockwave model. Especially at the end of the plasma plume expansion, where according to the drag model the plume plasma reaches the stopping distance.

Positions of the plasma plume top edge were measured for five values of applied laser pulse fluencies (figure 5). The data points in the figure 5 were fitted with drag model curves. Figure 5 shows that the plasma plume is larger for higher laser pulse fluences. The stopping distance calculated using the drag model equation varies from 125 μm to 210 μm for the laser pulse fluence ranging from 29 J/cm^2 to 52 J/cm^2. Also the expansion rate increases with laser fluence. This is expected since the increase in laser pulse fluence results in a higher initial plasma expansion velocity (measured at t = 0), which can be calculated from the drag model equation (2) as $V(t = 0) = R_{max} \cdot \beta$. The calculated initial plasma velocity as a function of laser fluence is presented in figure 6.

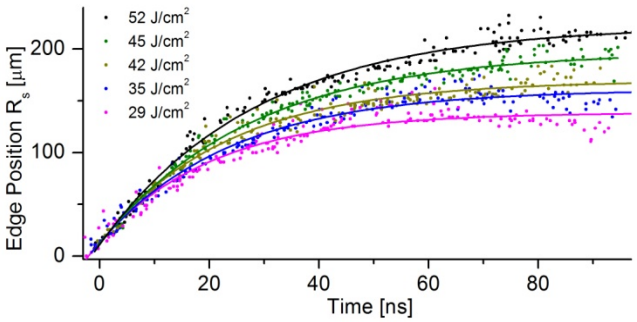

Fig. 5. Plasma plume top edge position for five values of laser pulse fluence

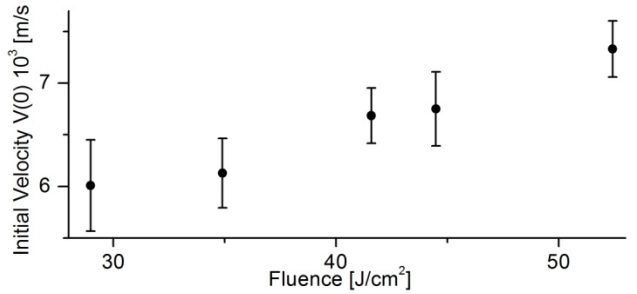

Fig. 6. Plasma initial velocity as a function of laser pulse fluence

Figure 6 shows that the initial plasma plume velocity rises from 6·10^3 m/s to 7·10^3 m/s with laser fluence increasing from 29 J/cm^2 to 52 J/cm^2. A similar value of the initial plasma plume velocity was obtained by Zhou et al. [10] who investigated the mechanism of silicon ablation with 200-ns laser pulses in air at atmospheric pressure, using the time-resolved technique. At a fluence of 40 J/cm^2, they determined the initial plasma velocity to be V (t=0) = 1,7·10^3 m/s, basing on the shockwave model. A slightly higher initial plasma plume velocity was obtained by Zeng et al. [19]. Using the laser shadowgraphy they estimated the vertical plasma plume expansion velocity to be 7.9·10^3 m/s., when the plasma was generated above silicon target in ambient air by a 5-ns UV (266 nm) laser pulse producing a fluence of 11 J/cm^2 on the target.

Conclusions

The early-stage expansion dynamics of the nanosecond laser pulse generated plasma plume in ambient air was experimentally investigated using the timed-resolved imaging. It was observed that the plasma plume was created in the form of a spot on the target surface. Next the plasma expands, resembling a mushroom-like shape and absorbs the laser pulse energy in the shielding process. The experimental results were compared with theoretical ones predicted by the shockwave and drag models. The comparison showed that the drag model better describes the plasma expansion in ambient air (i.e. at higher gas pressures). It was found that the initial velocity of the plasma (6-7·10^3 m/s) and stopping distance (125 μm – 210 μm) increased with laser pulse fluence.

REFERENCES

[1] Zhang Z., Gogos G., Effects of laser intensity and ambient conditions on the laser-induced plume, Appl. Surf. Sci., 252 (2005), 1057–1064

[2] Amoruso S., Toftmann B., Schou J., Velottaa R., Wanga X., Diagnostics of laser ablated plasma plumes, Thin Solid Films, 453 –454 (2004), 562–572

[3] Cristian Porneala C., Willis D.A., Time-resolved dynamics of nanosecond laser-induced phase explosion, J. Phys. D, 42 (2009), 155503–155510

[4] Jedynski M., Hoffman J., Mroz W., Szymanski Z., Plasma plume induced during ArF laser ablation of hydroxyapatite, Appl. Surf. Sci., 255 (2008), 2230-2236

[5] Toftmann B., Schou J., Dynamics of the plume produced by nanosecond ultraviolet laser ablation of metals, Phys. Rev. B, 67 (2003), 1041011–1041015

[6] Bhatti K.A., Khaleeq-ur-Rahman M., Jamil H., Latif A., Rafique M.S., Characterization of plasma propulsion by Nd:YAG laser, Vacuum, 84 (2010), 1080-1084

[7] Harilal S.S., Bindhu C.V., Tillack M.S., Najmabadi F., Gaeris A., Plume splitting and sharpening in laser-produced Aluminum Plasma, J. Phys. D, 35 (2002), 2935-2938

[8] Elhassan A., Abd Elmoniem H.M., Kassem A.K., Hairth M.A., Effect of applying static electric field on the physical parameters and dynamics of laser-induced plasma, J. Adv. Res., 1 (2010), 129–136

[9] Joshi H.C., Kumar A., Singh R.K., Prahlad V., Effect of a transverse magnetic field on the plume emission in laser-produced plasma: An atomic analysis, Spect. Act. B, 65 (2010) 415–419

[10] Zhou Y., Benxin W., Tao S., Forsman A., Gao Y., Physical mechanism of silicon ablation with long nanosecond laser pulses AT 1064nm through time-resolved observation, Appl. Surf. Sci., 257 (2011), 2886-2890

[11] Kononenko T.V., Garnov S.V., Klimentiv S.M., Konov V.I., Loubin E.N., Dausinger F., Raiber A., Taut C., Laser ablation of metals and ceramics in picosecond–nanosecond pulse width in the presence of different ambient atmospheres, Appl. Surf. Sci, 109/110 (1997), 48-51

[12] Karnakis D.M., High power single-shot laser ablation of silicon with nanosecond 355 nm, Appl. Surf. Sci, 252 (2006), 7823-7825

[13] Mao X., Wen S., Russo R.E., Time resolved laser-induced plasma dynamics, Appl. Surf. Sci., 253 (2007), 6316-6321

[14] Whitty W., Mosnier J.P., Diagnostic of an expanding laser-produced lithium plasma using ICCD frame photography and shadowgraphy, , Appl. Surf. Sci., 127-129 (1998), 1035-1040

[15] Taylor G.I., The formation of a blast wave by a very intense explosion, Proc. Roy. Soc. A, 201 (1950), 159-174

[16] Misra A., Thareja R.K., Investigation of laser ablated plumes using fast photography, IEEE Trans. Plasma Sci., 27 (1999), 1553-1558

[17] Callies G., Berger P., Hugel H., Time-resolved observation of gas-dynamic discontinuities arising during excimer-laser ablation and their interpretation, J. Phys. D, 28 (1995), 794–806

[18] Arnold N., Gruber J., Heitz J., Spherical expansion of the vapor plume into ambient gas: an analytical model, Appl. Phys. A, 69 (1999), 87– 93.

[19] Zeng X., Mao X., Grief R., Russo R.E., Ultraviolet femtosecond and nanosecond laser ablation of silicon: ablation efficiency and laser-induced plasma expansion, Proc. SPIE, 5448 (2004), 1150-1158

***Authors**: mgr. inż. Mateusz Tański, Instytut Maszyn Przepływowych PAN, ul. Fiszera 14, 80-231 Gdańsk, E-mail: tanski@imp.gda.pl; dr Marek Kocik, Instytut Maszyn Przepływowych PAN, ul. Fiszera 14, 80-231 Gdańsk, E-mail: kocik@imp.gda.pl; dr inż. Robert Barbucha, Instytut Maszyn Przepływowych PAN, ul. Fiszera 14, 80-231 Gdańsk, E-mail: brobert@imp.gda.pl; mgr. inż. Katarzyna garasz, Instytut Maszyn Przepływowych PAN, ul. Fiszera 14, 80-231 Gdańsk, E-mail: kgarasz@imp.gda.pl; prof. dr hab. inż. Jerzy Mizeraczyk, Instytut Maszyn Przepływowych PAN, ul. Fiszera 14, 80-231 Gdańsk, Akademia Morska, ul. ul. Morska 81-87, 81-225 Gdynia, E-mail: jmiz@imp.gda.pl.*